Relation between high-pressure spectroscopy and $f^{n-1}d^1$ excited-state geometry: A comparison between theoretical and experimental results in $SrF_2:Sm^{2+}$

José Luis Pascual*
Departamento de Química Física Aplicada, C-XIV, Universidad Autónoma de Madrid, 28049 Madrid, Spain

Zoila Barandiarán and Luis Seijo
Departamento de Química, C-XIV, and Instituto Universitario de Ciencia de Materiales Nicolás Cabrera, Universidad Autónoma de Madrid, 28049 Madrid, Spain

(Received 26 April 2007; published 20 September 2007)

In this paper, we present the results of *ab initio* model potential embedded-cluster calculations of Sm^{2+} impurities in SrF_2 in order to study the behavior of the electronic transitions of the dopant ion under high hydrostatic pressure. We find that the impurity-ligand bond length shortens upon $f \rightarrow d(e_g)$ excitation and, as a consequence, the $f \rightarrow d(e_g)$ transition energy decreases with increasing applied pressure. On the other hand, the bond lengths do not appreciably change upon $f \rightarrow f$ excitation and the energies of the $f \rightarrow f$ transitions are almost constant with pressure. These trends are in agreement with spectroscopic measurements under pressure in the title material, which gives credit to the computed bond length changes upon excitation, in contradiction with the widespread assumption of bond length lengthening upon $f \rightarrow d$ excitations. Spectroscopic experiments under high pressure are shown to be able to provide the sign of bond length changes in electronic transitions, constituting a simpler alternative to difficult excited-state x-ray absorption fine structure experiments.

DOI: 10.1103/PhysRevB.76.104109 PACS number(s): 71.55.−i, 62.50.+p, 71.10.−w, 61.72.Bb

I. INTRODUCTION

Recent *ab initio* studies of the structure and spectroscopy of complexes of lanthanide and/or actinide ions have shown that the bond length between the f element and the surrounding ligands shortens upon the lowest $f^n \rightarrow f^{n-1}d^1$ excitations.[1–3] This result is quite general, as it has been obtained for different halide ligands (F, Cl, Br), environments (crystals, liquid solutions, gas phase), oxidation states of the f element (III, IV), and number of f electrons.[1,2] However, it is in contradiction with the widespread assumption that the $f^n \rightarrow f^{n-1}d^1$ excitations lengthen the impurity-ligand bond distance. A direct experimental proof of the sign of the distortion upon excitation could be obtained by means of ground- and excited-state extended x-ray absorption fine structure (EXAFS) measurements. However, this kind of measurement is extremely demanding and, to our knowledge, no successful experiments for the excited states have been reported in the literature for f-element-doped solids or their complexes in liquid media.

As an alternative, it has been recently proposed that experimental spectroscopic studies under high hydrostatic pressure could be used to indirectly prove or reject the predicted bond length shortening upon the lowest $f^n \rightarrow f^{n-1}d^1$ excitations,[3] because quantum chemical simulations of pressure effects on $Cs_2NaYCl_6:(CeCl_6)^{3-}$, which included embedding effects, scalar relativistic effects, and dynamical electron correlation, have shown that the bond length shortening upon the $f^1 \rightarrow d(t_{2g})^1$ excitation and the predicted redshift of the $f^1 \rightarrow d(t_{2g})^1$ transition with pressure in this system are related.[3] The theoretical analyses[2,3] lead to the conclusion that the sign of the bond length change upon $i \rightarrow f$ excitation determines the sign of the slope of the transition energy with pressure:

$$\text{sign of } \frac{d\Delta E_e(i \rightarrow f)}{dP} = \text{sign of } \Delta R_e(i \rightarrow f). \quad (1)$$

As a consequence, the theoretically found sequence of bond lengths in octahedral complexes,[1] $R_e[f^{n-1}d(t_{2g})^1] \leq R_e[f^n] \leq R_e[f^{n-1}d(e_g)^1]$, should result in experimentally observable decreasing $f^n \rightarrow f^{n-1}d(t_{2g})^1$, constant $f^n \rightarrow f^n$, and increasing $f^n \rightarrow f^{n-1}d(e_g)^1$ transition energies with increasing hydrostatic pressure.

All this indicates that important structural information about the excited-state geometry can be inferred from measurable pressure-induced shifts, which is complementary to that obtained from the analyses of the transition band shapes alone, since the latter depend on the square of the bond length change.

It is therefore necessary to confirm or reject the theoretical predictions experimentally. It is also necessary to confirm or reject that they hold in more complex systems than the $4f^1$ open-shell Ce^{3+}-doped Cs_2NaYCl_6. Consequently, we take these two objectives as the goals of this paper.

For these purposes, Sm^{2+}-doped SrF_2 is a very suitable material: On the one hand, the luminescence of $SrF_2:Sm^{2+}$ has been measured as a function of pressure, up to 12 GPa,[4] as a probe of pressure-induced phase transitions in the host material. As a consequence, the sign of the slope $d\Delta E_e(i \rightarrow f)/dP$ is known for some emissions, which have been assigned to $4f^6 \rightarrow 4f^6$ and $4f^5 5d^1 \rightarrow 4f^6$ transitions. On the other hand, $4f^6$ Sm^{2+}-doped SrF_2 has a much more complicated electronic structure than Ce^{3+}-doped Cs_2NaYCl_6 and gives rise to a large number of states in the f^n and $f^{n-1}d^1$ manifolds with a large number of intrashell and intershell electronic interactions which have to be properly described in the calculations. Moreover, the different host provides a change in coordination, from sixfold octahedral

TABLE I. Effects of high pressure on the potential-energy surfaces of the different electronic states of $SrF_2:Sm^{2+}$. Distances are in Å, vibrational frequencies and energies are in cm^{-1}.

Lattice constant (a_0)	5.7960	5.7647	5.7334	5.6708	5.4825	5.1690
$-\Delta V/V$	0	0.0162	0.0324	0.0648	0.1623	0.3246
Pressure	1 bar	1.133 GPa	2.266 GPa	4.531 GPa	11.329 GPa	22.657 GPa
			Sm-F equilibrium distances (R_e)			
$4f^6\,{}^7A_{2g}$	2.513	2.504	2.491	2.466	2.390	2.264
$4f^6\,{}^5E_g$	2.516	2.506	2.494	2.469	2.393	2.266
$4f^5 5d(e_g)^1 1\,{}^7T_{2u}$	2.498	2.489	2.477	2.453	2.380	2.258
$4f^5 5d(t_{2g})^1 6\,{}^7T_{1u}$	2.545	2.536	2.523	2.499	2.427	2.300
$\langle 5d^1\rangle$[a]	2.526	2.517	2.505	2.481	2.408	2.283
			Sm–F bond length change upon excitation (ΔR_e)			
$4f^6\,{}^7A_{2g}\rightarrow 4f^6\,{}^5E_g$	0.003	0.002	0.003	0.003	0.003	0.002
$\rightarrow 4f^5 5d(e_g)^1 1\,{}^7T_{2u}$	−0.015	−0.015	−0.014	−0.013	−0.010	−0.008
$\rightarrow 4f^5 5d(t_{2g})^1 6\,{}^7T_{1u}$	0.032	0.032	0.032	0.033	0.037	0.036
$\rightarrow\langle 5d^1\rangle$[b]	0.013	0.013	0.014	0.015	0.018	0.019
			Breathing mode vibrational frequencies ($\bar{\nu}_{a_{1g}}$)			
$4f^6\,{}^7A_{2g}$	368	373	380	396	443	542
$4f^6\,{}^5E_g$	369	374	381	396	445	543
$4f^5 5d(e_g)^1 1\,{}^7T_{2u}$	370	376	383	399	448	549
$4f^5 5d(t_{2g})^1 6\,{}^7T_{1u}$	370	376	377	400	449	505
			Adiabatic transitions (ΔE_e)			
$4f^6\,{}^7A_{2g}\rightarrow 4f^6\,{}^5E_g$	16030	16050	16070	16110	16250	16610
$\rightarrow 4f^5 5d(e_g)^1 1\,{}^7T_{2u}$	16080	16000	15880	15640	14950	13940
$\rightarrow 4f^5 5d(t_{2g})^1 6\,{}^7T_{1u}$	31890	32110	32430	33070	35490	41250
$\rightarrow\langle 5d^1\rangle$[c]	25560	25660	25810	26100	27280	30330

[a] $R_e\langle 5d^1\rangle=[2R_e(1\,{}^7T_{2u})+3R_e(6\,{}^7T_{1u})]/5$.
[b] $\Delta R_e({}^7A_{2g}\rightarrow\langle 5d^1\rangle)=[2\Delta R_e(1\,{}^7T_{2u})+3\Delta R_e(6\,{}^7T_{1u})]/5$.
[c] $\Delta E_e({}^7A_{2g}\rightarrow\langle 5d^1\rangle)=[2\Delta E_e({}^7A_{2g}\rightarrow 1\,{}^7T_{2u})+3\Delta E_e({}^7A_{2g}\rightarrow 6\,{}^7T_{1u})]/5$.

(Cs_2NaYCl_6) to eightfold cubic (SrF_2), that inverts the effect of ligand field on the different electronic levels while keeping a high symmetry environment that allows one to calculate and draw potential-energy curves as a function of only one geometrical variable for different values of the applied external pressure. These curves cannot be easily drawn in low symmetry systems, a fact that makes the direct analyses of the bonding and its variation with pressure and electron excitation more difficult.

The calculations reported in this paper show that the excitation to the lowest-lying states of the $4f^5 5d(e_g)^1$ manifold, $4f^6\rightarrow 4f^5 5d(e_g)^1$, shortens the Sm-F bond distance and this is associated with a redshift of the $4f^6\rightarrow 4f^5 5d(e_g)^1$ transition energy with increasing pressure. This redshift has been, in fact, observed experimentally.[4] They also show that transitions to excited states of the $4f^6$ manifold do not appreciably change the bond distances so that $4f^6\rightarrow 4f^6$ transition energies virtually do not change with pressure. This result is confirmed experimentally.[4] Altogether, the results and their comparison with experimental data support the predicted bond length changes and confirm that high hydrostatic pressure spectroscopy is a technique valuable to give information about the geometry of excited states of f-element-doped ionic solids.

The paper is organized as follows: In Sec. II we present the details of the calculations. In Sec. III, we present the results and discussions. In Sec. IV, we present the conclusions of the paper.

II. DETAILS OF THE CALCULATIONS

The effects of hydrostatic pressure on the local structure and electronic transitions of the $(SrF_8)^{6-}$ defects in SrF_2 were studied using the relativistic *ab initio* model potential (AIMP) embedded-cluster method.[5,6] More detailed descriptions of the method as applied to f-element ions in ionic crystals can be found in Ref. 7. To incorporate scalar relativistic effects, we have used effective core potentials both for Sm and F. For Sm, we have used the [Kr]-core spin-free relativistic AIMP and the $(14s10p10d8f)$ Gaussian valence basis set of Ref. 8, augmented with a g function comprising three primitive functions whose exponents were obtained by maximum radial overlap with the Sm $4f$ orbitals. The final contraction pattern was $[6s5p6d4f1g]$. For F, we have used the [He]-core AIMP and the $(5s6p1d)$ valence basis set of Ref. 2. In order to incorporate dynamic electron correlation effects, complete active space self-consistent field

calculations[9] followed by multistate second order perturbation calculations (MS-CASPT2)[10,11] were done on a total of 20 and 22 electronic states with dominant $4f^6$ and $4f^5 5d^1$ electron configurations, respectively. The active space was generated by all possible configurations in which the 6 open-shell electrons occupy the 13 molecular orbitals of main character Sm $4f$, $5d$, and $6s$. Seventy-eight valence electrons of the $(SmF_8)^{6-}$ cluster were correlated in the MS-CASPT2 step. These electrons occupy the molecular orbitals of main character Sm $5s$, $5p$, $4f$, $5d$, $6s$ and F $2s$, $2p$. Large and uniform weights of the zeroth-order wave functions were obtained for all states and distances studied here in the intermediate single state CASPT2 calculations using an imaginary shift of 0.20.[12] The calculations presented here have been performed using the MOLCAS program system.[13]

The focus of this paper is on the trends of bond length changes and transition energies with increasing pressure and these trends have been shown to be very slightly affected by spin-orbit on a recent work on $Cs_2NaYCl_6:U^{3+}$ conducted in our laboratory.[14] Accordingly, all the numbers presented here correspond to spin-free Hamiltonian calculations. A detailed quantitative comparison of the absolute value of the calculated transition energies with experimentally determined transitions is out of the focus of this paper and it would require more demanding calculations with the inclusion of spin-orbit effects.

The effects of pressure were modeled by using AIMP embedding potentials produced in this work. The embedding potentials corresponding to a certain lattice constant, which are assigned to a given external pressure, were obtained through self-consistent embedded ions calculations;[6] they allow one to incorporate quantum-mechanical interactions with the host SrF_2 ions in the $(SmF_8)^{6-}$ cluster Hamiltonian. The values of the lattice constants used are listed in Table I, together with the corresponding $-\Delta V/V$ values. As the isothermal compressibility of the material is $\kappa=1.43$ kbar^{-1},[15] the used lattice constants are expected to span a pressure range of 1 bar–22.657 GPa, approximately. The actual embedding potential is built by adding to the cluster Hamiltonian AIMP embedding potentials for 1656 ions, located in a cube of length $5a_0$ centered on the impurity, plus 4888 additional point charges representing further ions (located in a cube of length $8a_0$). These ions bear the nominal ion charge, except those located at the frontier, which bear fractional charges according to Evjen's method.[16] All AIMP potentials (both core and embedding) and basis sets are available in electronic format from the authors.[17]

Sm^{2+} ions substitute for Sr^{2+} ions in the SrF_2 lattice, occupying sites of cubic symmetry $[SrF_2(O_h^5\text{-}F_{m3m})]$. We have calculated the embedded-cluster energies of a total of 42 electronic states of the $(SmF_8)^{6-}$ cluster at different Sm-F distances, for each lattice compression. We have studied 20 electronic states coming from the f^6 configuration, namely, those related to the ^7F ground-state term of the Sm^{2+} ion and some of the lowest-lying f^6 spin quintet states, especially those coming from the ^5D state of the Sm^{2+} ion. We have also studied the 22 lowest-lying spin septet states belonging to the f^5d^1 electron configuration: Those related to the $4f^5(^6H)5d(e_g)^1$, $4f^5(^6F)5d(e_g)^1$, and $4f^5(^6H)5d(t_{2g})^1$ (the eight lowest states) configurations of the Sm^{2+} ion. Plots of the potential-energy curves for the different states at ambient pressure can be found in Fig. 1. The results in Fig. 1 show three sets of states belonging, respectively, to the f^6, $f^5d(e_g)^1$, and $f^5d(t_{2g})^1$ electron configurations. All the states included in a particular manifold share very similar equilibrium distances and a_{1g} vibrational frequencies; this is true for all the different pressures studied here. For convenience and clarity, of all these states (42 in total), we will present only the results for the f^6 lowest spin septet ($^7A_{2g}$, ground state), f^6 lowest spin quintet (^5E_g), $f^5d(e_g)^1$ lowest spin septet ($1\,^7T_{2u}$), and $f^5d(t_{2g})^1$ lowest spin septet ($6\,^7T_{1u}$), as representatives of the different manifolds.

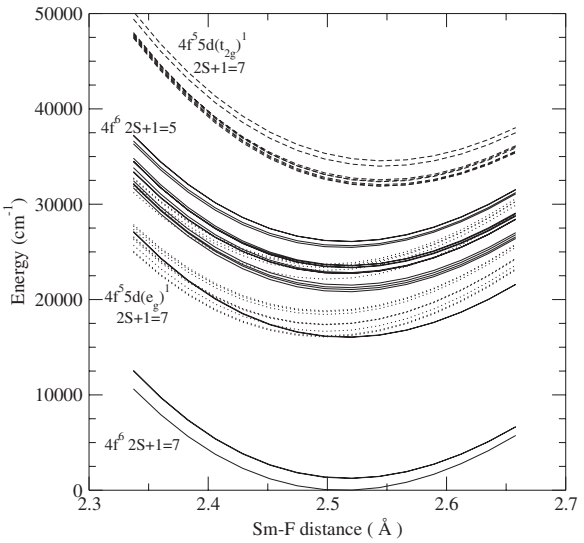

FIG. 1. Potential-energy curves of the different electronic states of $SrF_2:Sm^{2+}$ as a function of Sm-F distance in the a_{1g} mode (see text for details) at ambient pressure. Solid lines: $4f^6$ configuration, spin septet and quintet. Dotted lines: $4f^5 5d(e_g)^1$ configuration, spin septet. Dashed lines: $4f^5 5d(t_{2g})^1$ configuration, spin septet.

III. RESULTS AND DISCUSSION

For all 42 different electronic states mentioned above, we have computed the equilibrium distances (R_e), the shifts of the bond length upon excitation $[\Delta R_e(i \rightarrow j)]$, totally symmetric vibrational frequencies ($\bar{\nu}_{a_{1g}}$), and minimum-to-minimum transition energies $[\Delta E_e(i \rightarrow j)]$. We present the results for the selected representative states [$4f^6\,^7A_{2g}$, $4f^6\,^5E_g$, $4f^5 5d(e_g)^1 1\,^7T_{2u}$, and $4f^5 5d(t_{2g})^1 6\,^7T_{1u}$] in Table I and in Figs. 2 and 3.

The results of Table I and Fig. 2 show a redshift of the $4f^6\,^7A_{2g} \rightarrow 4f^5 5d(e_g)^1\ 1\,^7T_{2u}$ transition with pressure (of 95.8 cm^{-1}/GPa). Experimentally, the positions of the zero-phonon emission lines from the lowest $4f^5 5d(e_g)^1$ state and the $4f^6\,^5D_0$ state to the $4f^6\,^7F_1$ state have been determined.[4] The linear fit to experimental data is represented by solid lines in Fig. 2. The experiments predict a redshift of the $5d \rightarrow 4f$ band of some 149 cm^{-1}/GPa. It is clear from the figure that our calculated values reproduce the experimental

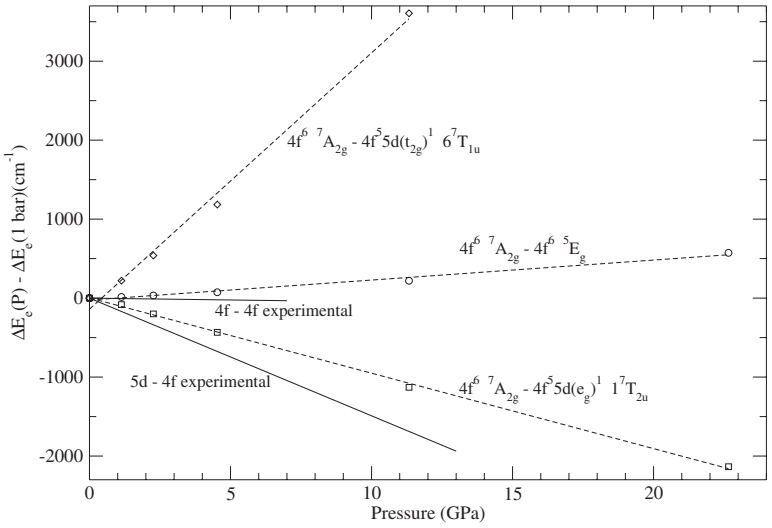

FIG. 2. Effects of pressure on the calculated minimum-to-minimum $4f^6\,{}^7A_{2g} \rightarrow 4f^6\,{}^5E_g$ (circles), $4f^6\,{}^7A_{2g} \rightarrow 4f^5 5d(e_g)^1\ 1\,{}^7T_{2u}$ (squares), and $4f^6\,{}^7A_{2g} \rightarrow 4f^5 5d(e_g)^1\ \ 6\,{}^7T_{1u}$ (diamonds) transition energies. Dashed lines: Least-squares linear fits to the calculated transitions. Solid lines: Least-squares linear fits to the experimentally obtained data (see Ref. 4).

trend. This agreement confirms the theoretically predicted shifts of the transition energies with pressure, the remaining quantitative discrepancies being associated with the approximations adopted in the present work, commented above.

The plots of the potential-energy surfaces of the different states for ambient pressure and 11.329 GPa are given in Fig. 3. The results in Table I and Fig. 3 show a significant shortening of the Sm–F bond length upon $4f^6\,{}^7A_{2g} \rightarrow 4f^5 5d(e_g)^1\ 1\,{}^7T_{2u}$ excitation at ambient pressure as well as at higher pressures. These results are in line with those found before for electronic transitions in sixfold coordinated Ce^{3+}, that is, a shortening of the bond length upon excitation from f to the lowest-lying d orbitals (t_{2g} in octahedral coordination, e_g in cubic coordination). As stated above, the shortening of the Sm–F bond length upon $4f^6\,{}^7A_{2g} \rightarrow 4f^5 5d(e_g)^1\ 1\,{}^7T_{2u}$ excitation is related to a redshift of the transition with pressure, confirmed experimentally. From these facts, we conclude that Eq. (1) also holds in this more complex six f-electron system.

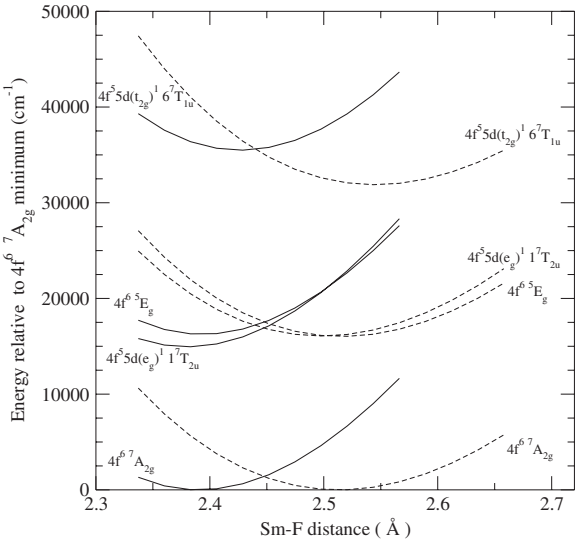

FIG. 3. Effects of pressure on the potential-energy curves of the different electronic states of $SrF_2:Sm^{2+}$. Dashed lines: Ambient pressure. Solid lines: High pressure (11.329 GPa).

On the other hand, the results of Table I and Fig. 2 show a small blueshift of the $4f^6\,{}^7A_{2g} \rightarrow 4f^6\,{}^5E_g$ transition with pressure of 25.3 cm^{-1}/GPa. The experiments predict a negligible redshift of the $4f \rightarrow 4f$ band (3.9 cm^{-1}/GPa).[4] Again, our results reproduce the experimental trend of almost independence of the $4f \rightarrow 4f$ transition energy with pressure. The results in Table I and Fig. 3 show a negligible increase of the bond length upon $4f^6\,{}^7A_{2g} \rightarrow 4f^6\,{}^5E_g$ excitation. This negligible increase of the bond length is related to a transition energy nearly constant with pressure.

Altogether, these results give a strong support to the theoretically predicted bond length changes upon $f \rightarrow d$ excitation. On the other hand, they firmly establish high-pressure spectroscopy experiments as a way to find the sign of bond length changes upon excitation in these systems.

The results in Table I and Fig. 3 show a bond length increase upon $4f^6\,{}^7A_{2g} \rightarrow 4f^5 5d(t_{2g})^1\ 6\,{}^7T_{1u}$ excitation. From the results in Table I and Fig. 2, we see that this transition shifts to higher energy with increasing pressure (slope: 324.5 cm^{-1}/GPa). This fact is predicted by Eq. (1), in line with the results of Ref. 3 and completes the picture for the relative positions of the different states in eightfold cubic coordination: $R_e[f^{n-1}d(e_g)^1] \leqslant R_e[f^n] \leqslant R_e[f^{n-1}d(t_{2g})^1]$. As in sixfold octahedral coordination, the transition to the lowest-lying $4f^{n-1}5d^1$ states shortens the impurity-ligand bond length and the transition to the highest-lying $4f^{n-1}5d^1$ states lengthens it. This bond length shifts result in decreasing $4f^n \rightarrow 4f^{n-1}5d(e_g)^1$, nearly constant $4f^n \rightarrow 4f^n$, and increasing $4f^n \rightarrow 4f^{n-1}5d(t_{2g})^1$ transition energies with increasing hydrostatic pressure. The first two have been contrasted with experiment. There are no experimental data on the variation of the $f^n \rightarrow f^{n-1}d(t_{2g})^1$ transition energy with pressure (it has been measured only at ambient pressure[18]).

Using the values for the calculated $4f^6\,{}^7A_{2g} \rightarrow 4f^5 5d(e_g)^1\ 1\,{}^7T_{2u}$ and $4f^6\,{}^7A_{2g} \rightarrow 4f^5 5d(t_{2g})^1\ 6\,{}^7T_{1u}$ excitations, we can define the bond length and the energy of the baricenter state of the $4f^5 5d$ configuration as the weighted averages of the values for the $4f^5 5d(e_g)^1\ 1\,{}^7T_{2u}$ and $4f^5 5d(t_{2g})^1\ 6\,{}^7T_{1u}$ states.

These values, for the different pressures, are shown in Table I under the heading $\langle 5d^1 \rangle$. Although this state is not real, it is useful as a reference for discussion, as it corresponds to a removal of the *d* ligand field splitting effects. According to our calculations, the $4f^n \rightarrow \langle 4f^{n-1}5d^1 \rangle$ transition results in a lengthening of the impurity-ligand bond length, the final shortening of the bond length upon $4f^n \rightarrow 4f^{n-1}5d(e_g)^1$ transition being due to the ligand field splitting of the 5*d* orbitals. This is the same effect found in Ref. 2 for $(CeF_6)^{3-}$ embedded in an elpasolite lattice. Related to this lengthening of the impurity-ligand bond length upon $4f^n \rightarrow \langle 4f^{n-1}5d^1 \rangle$ transition, the energy of the (hypothetical) $4f^n \rightarrow \langle 4f^{n-1}5d^1 \rangle$ transition should grow with increasing pressure.

Although the general agreement of our calculated transition energy slopes versus pressure with the experimental ones is satisfactory (see Fig. 2), we notice that our calculated redshifts are smaller than the experimental ones. In fact, for the $f \rightarrow f$ transition we predict a small blueshift, while experimentally a negligible redshift is found (see Fig. 2). Spin-orbit can have an influence on the slopes of the transition energies, as it will mix states with slightly different Sm-F distance. As a way to have a hint of what could be the influence of spin-orbit on the calculated slopes, we have calculated the slope of the transition energy versus pressure for all the states considered in the calculations (see above) and then calculated the averages of the slopes of transition energies for the different manifolds. We consider that spin-orbit will couple states mainly within these different manifolds and the comparison of these averaged slopes gives a hint on the spin-orbit effects on these values. The calculated averages are 39.8 cm^{-1}/GPa (transition to states in the $4f^6$ $S=3$ manifold), 27.2 cm^{-1}/GPa ($4f^6 S=2$ manifold), −80.8 cm^{-1}/GPa [$4f^5 5d(e_g)^1$ manifold], and 328.2 cm^{-1}/GPa [$4f^5 5d(t_{2g})^1$ manifold]. Then, using these numbers we get a value of −12.6 cm^{-1}/GPa for the slope of the transition energy versus pressure of the $4f^6$ $S=3 \rightarrow 4f^6$ $S=2$ excitations. The sign of this slope is affected by the inclusion of spin-orbit effects, and accordingly, we can only state that the transition energy is almost constant as pressure changes, in qualitative agreement with experiment.

Experimentally, the values of the transition from the lowest level of the $4f^5 5d(e_g)^1$ configuration to the ground state and the transition from the $^5D_0$ state of the $4f^6$ configuration (the lowest-lying quintet state) to the ground state have been determined, at ambient pressure, to be 15 032 and 14 605 cm^{-1}, respectively.[4] Our results for the position of the lowest-lying $4f^5 5d(e_g)^1$ state and the lowest-lying $4f^6$ quintet state are, respectively, 16 080 and 16 030 cm^{-1}. The difference between these numbers leaves room for the effects not considered in the calculation, mainly spin-orbit interaction and a higher level of electron correlation. An accurate calculation of the absolute value of the transitions is not the goal of this paper and it would require very demanding calculations.

On the other hand, our results at ambient pressure for the totally symmetric vibrational frequencies could be compared with experimental ones, as they should be almost unaffected by spin-orbit effects.[7,14,19] $SrF_2:Sm^{2+}$ has been shown to be a laser[20] and its ambient-pressure absorption,[20,21] fluorescence,[21] excited-state absorption,[18] and hole burning[22] spectra have been reported in the literature. Wood and Kaiser[21] reported progressions of peaks in the emission spectrum of $Sm^{2+}:SrF_2$ that they assigned to vibrational structure of the electronic transitions. The highest of these progressions has an average spacing of 349 cm^{-1} and should be due to the totally symmetric a_{1g} vibrational mode. Our value of 368 cm^{-1} for this frequency in the $^7A_{2g}$ ground state compares favorably with experiment. The overestimation of around 6% is in line with previous results.[7]

Finally, let us remark the fact that the rule of thumb derived in Ref. 3 to predict the sign of the change of a transition with pressure, based on calculations on octahedral Ce^{3+} clusters ($4f^1$) (use the configurational diagram for ambient pressure and assume that the effects of pressure correspond to moving inward across the *R* axis), can be equally used in this case (cubic $4f^6$ ion), as it can be deduced from Fig. 3.

IV. CONCLUSIONS

In this paper, we present quantum-mechanical *ab initio* simulations of high hydrostatic pressure spectroscopic experiments on $Sm^{2+}:SrF_2$. The simulations have been carried out using embedded-cluster wave-function based techniques which include scalar relativistic effects, valence electron correlation, and quantum-mechanical embedding effects. We have obtained spectroscopic constants (equilibrium distances and breathing mode vibrational frequencies) for a number of states of the impurity and calculated minimum-to-minimum transition energies between the states, for several external pressures. We have found that the relative bond length positions are $R_e[f^{n-1}d(e_g)^1] \leqslant R_e[f^n] \leqslant R_e[f^{n-1}d(t_{2g})^1]$ in this cubic symmetry. In line with previous theoretical results[3] that have not been confirmed nor rejected experimentally, this sequence of bond lengths leads to a redshift in $4f^n \rightarrow 4f^{n-1}5d(e_g)^1$ transitions, nearly constant $4f^n \rightarrow 4f^n$ transition energies, and a blueshift in $4f^n \rightarrow 4f^{n-1}5d(t_{2g})^1$ transitions with increasing applied pressure. In $Sm^{2+}:SrF_2$, these trends are qualitatively the same as those found in actual experimental results,[4] the quantitative agreement of the slopes of the transition energy versus pressure being satisfactory. This agreement gives a substantial amount of credit to the theoretical determinations of bond length changes upon excitation on complexes of *f* elements and, in particular, establishes the fact that a shortening of the bond length happens upon the lowest $f^n \rightarrow f^{n-1}d^1$ transitions. Besides, it is shown that high-pressure spectroscopic experiments can indirectly reveal the sign of the bond length changes upon electronic excitation, constituting a simpler alternative to highly demanding excited-state EXAFS experiments.

ACKNOWLEDGMENTS

This work has been partly supported by Ministerio de Educación y Ciencia, Spain, under Contract No. CTQ2005-08550.

*joseluis.pascual@uam.es

[1] Z. Barandiarán and L. Seijo, J. Chem. Phys. **119**, 3785 (2003).
[2] Z. Barandiarán, N. M. Edelstein, B. Ordejón, F. Ruipérez, and L. Seijo, J. Solid State Chem. **178**, 464 (2005).
[3] F. Ruipérez, L. Seijo, and Z. Barandiarán, J. Chem. Phys. **122**, 234507 (2005).
[4] C. S. Yoo, H. B. Radousky, N. C. Holmes, and N. M. Edelstein, Phys. Rev. B **44**, 830 (1991).
[5] Z. Barandiarán and L. Seijo, J. Chem. Phys. **89**, 5739 (1988).
[6] L. Seijo and Z. Barandiarán, in *Computational Chemistry: Reviews of Modern Trends*, edited by J. Leszczynski (World Scientific, Singapore, 1999), Vol. 4, p. 55.
[7] L. Seijo and Z. Barandiarán, J. Chem. Phys. **118**, 5335 (2003).
[8] L. Seijo, Z. Barandiarán, and B. Ordejón, Mol. Phys. **101**, 73 (2003).
[9] B. O. Roos, P. R. Taylor, and P. E. M. Siegbahn, Chem. Phys. **48**, 157 (1980); P. E. M. Siegbahn, A. Heiberg, J. Almlöf, and B. O. Roos, J. Chem. Phys. **74**, 2384 (1981); P. Siegbahn, A. Heiberg, B. Roos, and B. Levy, Phys. Scr. **21**, 323 (1980).
[10] J. Finley, P.-Å. Malmqvist, B. O. Roos, and L. Serrano-Andrés, Chem. Phys. Lett. **288**, 299 (1998).
[11] A. Zaitsevskii and J. P. Malrieu, Chem. Phys. Lett. **233**, 597 (1995).
[12] N. Forsberg and P.-Å. Malmqvist, Chem. Phys. Lett. **274**, 196 (1997).
[13] G. Karlström, R. Lindh, P.-Å. Malmqvist, B. O. Roos, U. Ryde, V. Veryazov, P.-O. Widmark, M. Cossi, B. Schimmelpfennig, P. Neograd y, and L. Seijo, Comput. Mater. Sci. **28**, 222 (2003).
[14] F. Ruipérez, Z. Barandiarán, and L. Seijo (unpublished).
[15] G. A. Samara, Phys. Rev. B **13**, 4529 (1976).
[16] H. M. Evjen, Phys. Rev. **39**, 675 (1932).
[17] Detailed core and embedding AIMP data libraries in electronic format are available from the authors upon request or directly at the address http://www.uam.es/quimica/aimp/Data/-AIMPLibs.html
[18] S. A. Payne, L. L. Chase, W. F. Krupke, and L. A. Boatner, J. Chem. Phys. **88**, 6751 (1988).
[19] B. Ordejón, M. Karbowiak, L. Seijo, and Z. Barandiarán, J. Chem. Phys. **125**, 074511 (2006).
[20] P. P. Sorokin, M. J. Stevenson, J. R. Lankard, and G. D. Pettit, Phys. Rev. **127**, 503 (1962).
[21] D. L. Wood and W. Kaiser, Phys. Rev. **126**, 2079 (1962).
[22] R. M. Macfarlane and R. S. Meltzer, Opt. Commun. **52**, 320 (1985).